A Realistic Stress Transfer Model for Geogrids in Pullout

G. E. Bauer & Y. Zhao
Carleton University, Ottawa, ON, Canada

ABSTRACT: Fifteen pullout tests using two types of geogrids were carried out in a large tank. The interaction behaviour of the grids with two granular soils were determined. Numerical analyses for tensile force and shear stress distributions along the embedded grid are proposed considering the physical properties of the mesh and the soil. The experimental values compared well with the corresponding data from the numerical procedure.

1 INTRODUCTION

The pullout resistance , or anchorage capacity, of a geogrid is an important consideration in a stability analysis of a reinforced earth structure. A pullout apparatus is commonly used to determine the anchorage capacity of the specified reinforcing element. In a standard test little information is obtained about the load transfer mechanism or how the tensile forces are distributed along the reinforcement. The load transfer between soil and reinforcement depends on several factors, such as physical and geometric properties of the geogrid, soil type, boundary and stress conditions, as well as rate of strain application.

In order to investigate the factors affecting the anchorage capacity of several geogrids in various granular soils, pullout tests were carried out in a large apparatus (1.55 m long by 0.9 m wide by 1.25 m high). The free - end displacement together with the applied pullout force were monitored. In addition, the corresponding displacements of nodal points and the embedded end of the geogrid were measured. Based on these measurements, the average strains, tensile forces and interfacial shear forces between grid junctions were calculated. Fifteen pullout tests were performed in total in order to evaluate the various parameters.

Several methods of numerical analysis are proposed to estimate the mobilised tensile forces along the geogrid and the shear stress distribution at the soil grid interface considering soil and geogrid properties. The numerical methods required input data from independent laboratory tests.

In general good agreement was obtained between the experimental results and the corresponding values from the numerical analysis.

2 EXPERIMENTAL PROGRAM

2.1 Test apparatus

The pullout apparatus consisted of a large concrete tank, a pullout mechanism (actuator with load cell), a vertical load application System, and a data acquisition and test control system. A detailed description of the test setup was given by Bauer and Shang (1993). A schematic diagram including the overall dimensions of the test rig is shown in Fig. 1. The whole system was fully automated. A test was terminated after the pullout force reached a residual value or the free-end displacement of the geogrid had reached a value of 75 mm.

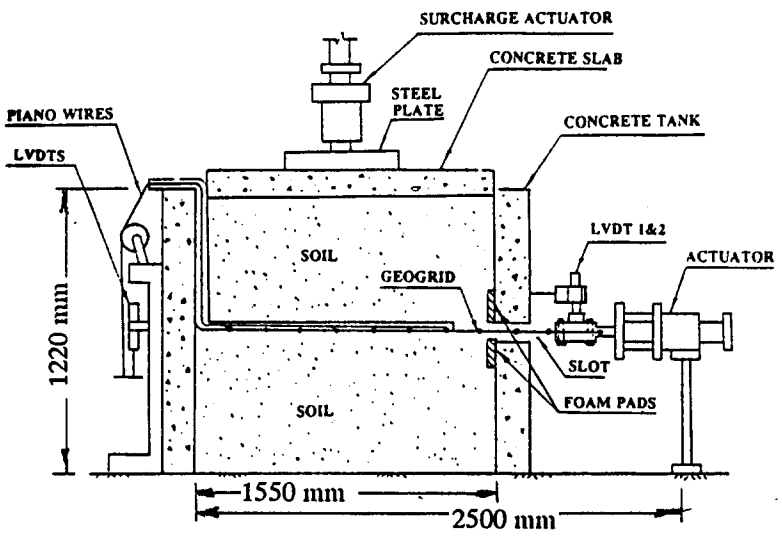

Fig. 1 Diagram of pullout apparatus

2.2 Soil properties

Two granular soils were investigated in conjunction with the geogrids, a uniform coarse sand and a well-graded crushed limestone aggregate. The sand had a mean grain size of 0.35 mm and was placed in 150 mm lifts into the tank. The dry density of the sand was 19.8 kN/ m^3 (modified Proctor) with a moisture content of 11 % and was compacted into the tank having a density of 18.0 kN/ m^3 with a moisture content of 8 % corresponding to 95 % compaction effort. The peak and residual angles of internal friction were 46.0^0 and 36.8^0, respectfully.

The well-graded crushed limestone aggregate had a mean particle size of 3.5 mm and a maximum diameter of 20 mm. The modified Proctor compaction test yielded a maximum dry density of 22.0 kN/ m^3 with an optimum water content of 6.8 %. The in-place density, corresponding to 95 % of modified Proctor compaction, was 19.2 kN/ m^3 having a water content of 4 %. Internal friction angles of the in-place soil were 52.0^0 and 43.1^0 for peak and residual values, respectfully.

The stress-strain relationship of the two soils are shown in Fig. 2.

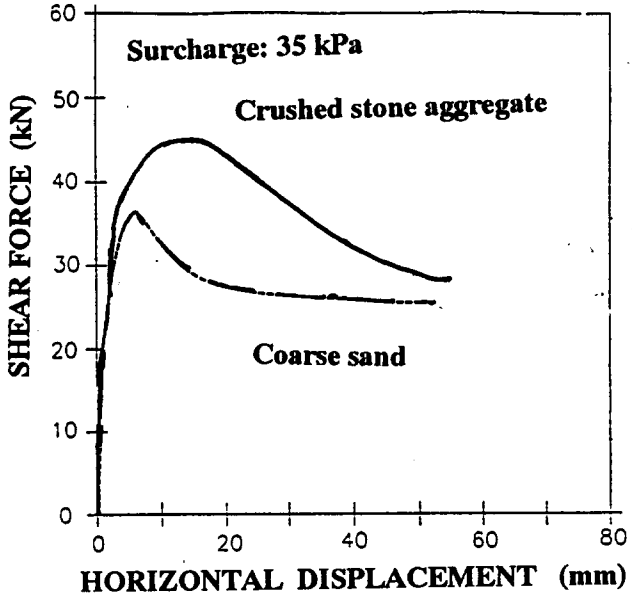

Fig. 2 Stress-strain response of the two test soils

2.3 Geogrids

The two geogrids investigated were an extruded uniaxial polyethylene mesh (TENSAR UX 1500) and a knotted or woven polypropylene grid (CONWED 9027). The physical properties, as determined in laboratory tests are summarised in Table 1.

The stress-strain properties of 0.75m and of 0.40 m wide grid specimens both having a length of 1.5m were determined in the laboratory and were found to be the same.

Table 1 Mechanical properties of geogrids

Type	Tensile Strength (kN/m)	Strain (%)	Comment
TENSAR	88.3	11.2	mean
	3.8	1.5	stand. deviation
CONWED	86.2	14.5	mean
	1.8	0.8	stand. deviation

2.4 Test procedure

The horizontally placed geogrid specimen (Fig. 1) was consolidated under the specified surcharge and then pulled through the soil at a rate of 1 mm/min. This rate of pullout has been generally adopted by most researchers (Ingold, 1983; Mowafy, 1986; Palmeira, 1987). The load-deformation response, the displacement of nodal points and any vertical deformation were recorded by the data acquisition system.

3 NUMERICAL PROCEDURE

3.1 Pullout force-deformation response and shear stress

The numerical model is based on the measurement of nodal displacements of the geogrid knowing the soil parameters and the physical and geometric properties of the geogrid. The grid was discretisized into a series of elements and each grid element is assumed to behave as an stical spring. The interface friction between the soil as well the bearing resistance of the transverse members of the grid is also taken into consideration. The constitutive behaviour governing the pullout force in relation to the front-end displacement of the geogrid was derived by Zhao (1993) as

$$F_0 = E A_c \sqrt{2\alpha [y_0 - B \ln (B + y)] - \alpha B \ln B} \quad (1)$$

where F_0 is the pullout force, E the elastic modulus of the grid, A_c the cross-sectional area, α is the area ratio between geogrid and soil and B is a constant to be determined experimentally from a sliding test.

The shear stress distribution along the embedded part of the mesh was also given by (Zhao, 1993) as

$$\tau (x) = A Y / (B+Y) \quad (2)$$

where Y is the shear displacement at point x, A and B are constants to be determined from a geogrid sliding test.

The relation between the pullout behaviour of the grid and the displacement can be approximated by a flow rule analysis. In pullout part of the energy is dissipated by friction and bearing failure of the soil and part is stored as elastic energy within the geogrid. This can be written as

$$\delta E = f_b B\ \delta x + 1/2 \int_0^l \sigma\ \varepsilon\ A_c\, dx \qquad (3)$$

where δE is the energy dissipated, δx is the relative movement (slip) between the soil and the reinforcement, N is the normal load and f_b is the bond coefficient which has to determined from a sliding test. σ and ε are the tensile stress and strain in the reinforcement, respectfully. A_c and l are the area and the the corresponding embedded length of the geogrid.

The total work done by the pullout force is given by

$$W_T = \int dF\ (\Delta x) \qquad (4)$$

In the above equation (4), W_t is taken as the total work done by the system as represented by the area under the pullout force- displacement reationship. The negative work done by the dilating soil has been considered minimal and was neglected. The advantage of the flow rule technique over a limit equlibrium analysis is that it will take the whole force-displacement response into account instead of selecting one point on the curve only, generally the peak value.

4 RESULTS AND DISCUSSION

4.1 Pullout resistance

The most important factor governing the pullout resistance (anchorage capacity), besides the properties of the soil, is the extensibility and the geometry of the geogrid. For a completely rigid reinforcing element the displacement would be the same at any point along the grid producing a uniform shear stress distribution. All commercially available geogrids should be considered extensible and thereby causing non-uniform interaction stresses. Fig 3 shows the result of a pullout test in the uniform coarse sand together with the prediction from the numerical model. The agreement is quite good. A similar comparison is given in Fig. 4 for the well-graded limestone aggregate. At large displacements (> 80 mm) the model will overpredict the pullout resistance. This is probably due that with continued grid displacement the larger particles will have been relocated away from the geogrid resulting in a decrease of particle interlock and thereby decreasing the shear resistance.

4.2 Geogrid extensibility and nodal displacement

Fig. 5 demonstrates the effect of geogrid extensibility or elastic modulus on the pullout resistance. It is apparent that with an increase in grid stiffness the pullout resistanse is increased for a given displacement. The analysis assumes

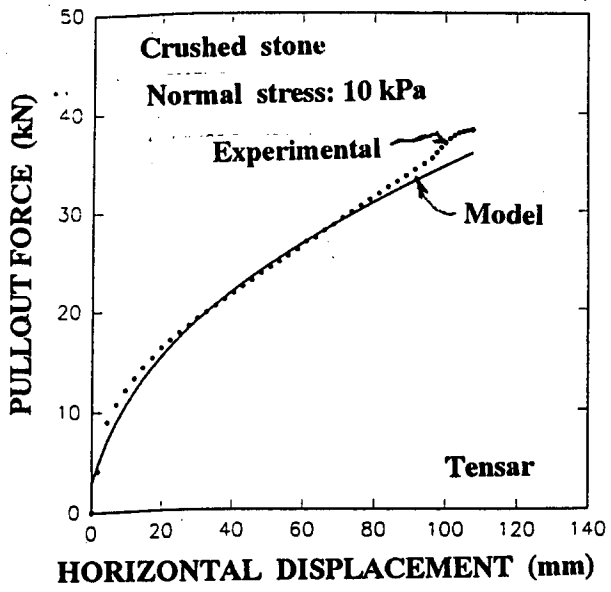

Fig. 3 Numerical and test results of pullout (coarse sand)

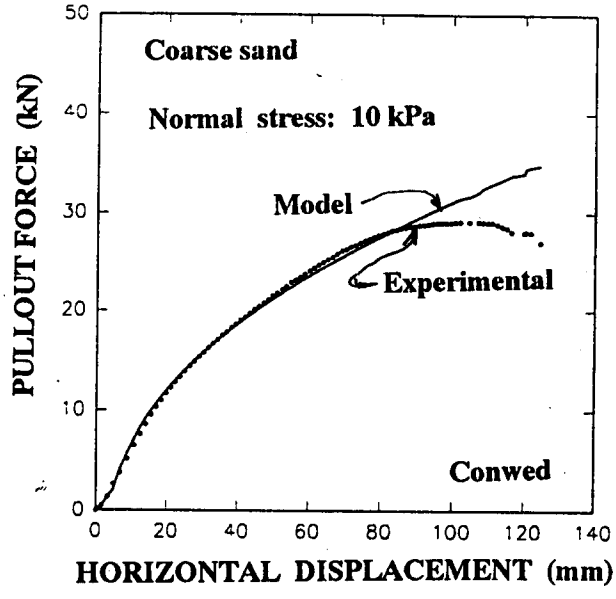

Fig. 4 Numerical and test results of pullout (crushed stone)

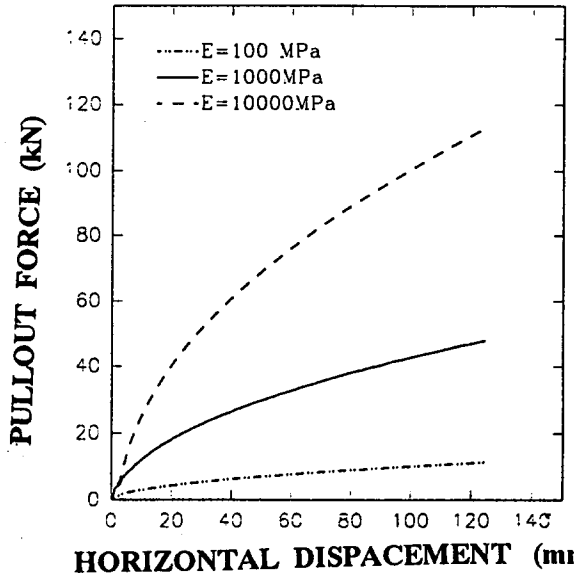

Fig. 5 Effect of grid extensibility on pullout force

that complete bonding between geogrid and soil exists and the bond strength is not exceeded. The measured and calculated nodal displacement along the geogrid is given in Fig. 6 for the maximum pullout resistance. The calculated values are determined for various reinforcement stiffnesses. The displacement distribution is similar to those measured by Bauer and Shang (1993) and Farrag and Griffin (1993).

4.3 Pullout resistance and shear stress distribution

The predicted and measured tensile force distribution along the geogrid for the peak or maximum pullout force is shown in Fig. 7 for Tensar geogrid placed in the coarse sand. The agreement is quite good. Similar comparisons were made for intermediate applied pullout forces yielding equally good agreement. For pullout forces beyond peak the agreement was fair, especially toward the embedded end of the mesh. Geogrids embedded in the well-graded limestone aggregate compared less favourably close to peak and beyond peak values. Again, a possible explanation for that behaviour could be that a rearrangement of the coarser particles will occur with continued grid displacement.The theoretical shear stress distribution (equation 2) along the embedded length of the grid is shown in Fig. 8 together with the experimental values. The agreement is quite good.

5 CONCLUSIONS

The pullout resistance of a geogrid embedded in a soil is a function of the soil parameters, the grid properties and the soil stresses. It is essential that not only the front-end displacement in conjunction with the applied force is monitored, but also the displacement of nodal points along the embedded part of the mesh. The results from the numerical methods yielded good agreement with the corresponding experimental values and could therefore be used as a first step in predicting design parameters.

REFERENCES

Bauer , G. E. and Shang, Q. (1980) Pullout resistance of large geogrid specimens in site specific soils, *Geotechnical Engineering Journal,* 23, 1:17-37.

Farrag, K. A. and Griffin, P. (1993) Pullout testing of geogtrids in cohesive soils, *Geosynthetic soil reinforcement testing procedures,*ASTM, STP,1190, 77-89.

Ingold, T. S. (1983) Laboratory testing of geogrid reinforcement in sand, *Geotechnical Testing Journal,* 6:, 101-111.

Mowafy, Y. M. (1987) Analysis of grid reinforced earth structures, *Ph. D. thesis,* Civil Engineering, Carleton University, Ottawa, Canada.

Palmeira, E. M. (1987) The study of soil-reinforcement interaction by means of large scale tests, *Ph.D. thesis, University of Oxford, England.*

Zhao, Y. (1993) Strength and deformation behaviour of geogrid reinforced soils, *Ph. D. thesis,* Civil Engineering, Carleton University, Ottawa, Canada.

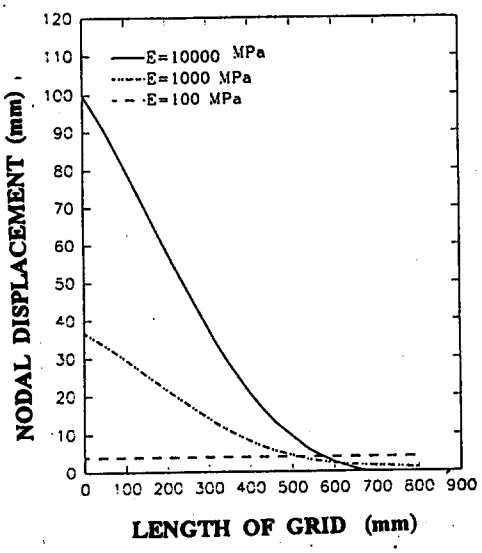

Fig. 6 Effect of grid extensibility on nodal displacement

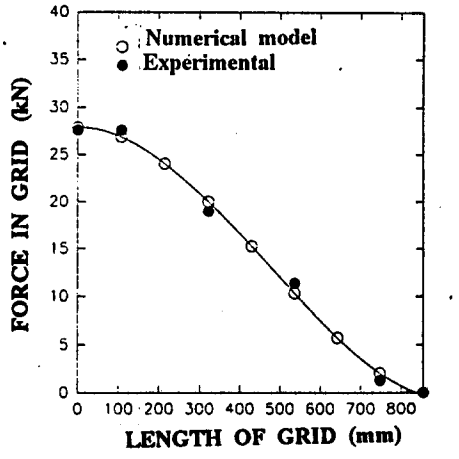

Fig. 7 Tensile force distribution at maximum pullout

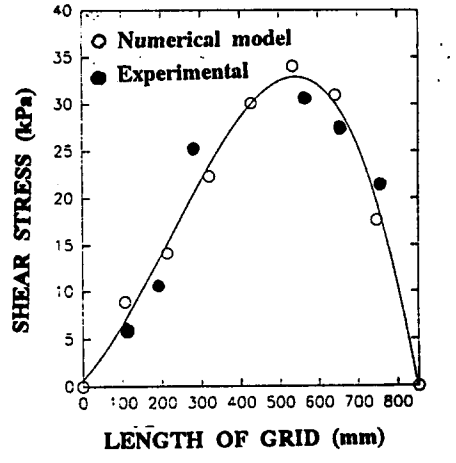

Fig. 8 Shear stress distribution at maximum pullout